Published in final edited form as:
IEEE Trans Biomed Eng. 2011 March ; 58(3): 521–530. doi:10.1109/TBME.2010.2096424.

Closed-Loop Identification: Application to the Estimation of Limb Impedance in a Compliant Environment

David. T. Westwick[Member, IEEE] and
Department of Electrical and Computer Engineering, Schulich School of Engineering at the University of Calgary. 2500 University Dr. NW, T2N 1N4, Canada

Eric J. Perreault[Member, IEEE]
Department of Biomedical Engineering and the Department of Physical Medicine and Rehabilitation at Northwestern University. He also has an appointment in the Sensory Motor Performance Program, Rehabilitation Institute of Chicago, 345 E. Superior, Chicago, IL, 60611, USA

David. T. Westwick: dwestwic@ucalgary.ca; Eric J. Perreault: e-perreault@northwestern.edu

Abstract

The force and position data used to construct models of limb impedance are often obtained from closed-loop experiments. If the system is tested in a stiff environment, it is possible to treat the data as if they were obtained in open loop. However, when limb impedance is studied in a compliant environment, the presence of feedback cannot be ignored. While unbiased estimates of a system can be obtained directly using the prediction error method, the same cannot be said when linear regression or correlation analysis are used to fit nonparametric time- or frequency domain models. We develop a prediction error minimization based identification method for a nonparametric time-domain model augmented with a parametric noise model. The identification algorithm is tested on a dynamic mass-spring-damper system, and returns consistent estimates of the system's properties under both stiff and compliant feedback control. The algorithm is then used to estimate the impedance of a human elbow joint in both stiff and compliant environments.

Index Terms

System Identification; Limb Impedance; Joint Dynamics; Separable Least Squares; Noise Model; ARMA

I. Introduction

System identification, the construction of mathematical models of dynamic systems from input/output measurements, has been extensively used to characterize limb impedance, defined as the dynamic relationship between position and force. Typically, an actuator is used to control the position of a single joint or multiple joints within the same limb. The actuator moves the joint through a prescribed series of motions, while the imposed displacements and corresponding forces are measured. System identification techniques are then used to fit dynamical models between the measured force(s) and displacement(s).

The actuator is often configured as a closed-loop position servo. It is supplied with a position command, and applies forces to the limb in such a way that the limb tracks the

Correspondence to: David. T. Westwick, dwestwic@ucalgary.ca.

desired trajectory. Thus, the dynamics of the limb must be estimated using data that were gathered in a feedback loop, thereby complicating the system identification process.

One approach to this problem involves using an actuator that is much stiffer than the joint that is being studied [1]. If the position of the joint is considered to be the system input, and that input is under direct control (via the stiff actuator), then the feedback has been effectively broken and the data can be treated as if they were gathered in open-loop conditions. Experiments such as this have been used to construct quasi-linear models of the impedance of individual [2]–[4] and multiple [5]–[7] joints under a variety of conditions.

In contrast to the control systems literature, where low-order parametric models are most commonly used, studies of limb impedance typically use nonparametric models in either the time or frequency domain to reduce the number of *a priori* assumptions made about the system structure. For example, in the time domain, finite impulse response (FIR) filters are often used to represent linear (or quasi-linear) systems, as their identification requires very little *a priori* information: typically just an upper bound on the memory length of the system. Furthermore, these nonparametric models can be readily extended to include certain types of nonlinearities. Indeed by using appropriately chosen block structured models, it has been possible to include the effects of reflexes in these models [8].

While this approach has been used successfully, it is suitable only for interactions with stiff environments and generally cannot be used to investigate limb mechanics during the vast repertoire of tasks that involve interactions with more compliant environments. More recent experiments have sought to characterize limbs as they interact with compliant environments [9]–[12], those that can be displaced when the limb applies a force. Under these conditions, the feedback through the actuator can no longer be ignored. Thus, the identification must be performed using closed-loop data, and employ techniques that will not be biased by the effects of the feedback.

Earlier studies [9], [10] employed transient inputs, and studied the responses directly without attempting to identify a model from the closed-loop data. More recently, system identification techniques have been used to construct non-parametric models in both the time [12] and frequency [11] domains. These studies both employed instrumental variable (IV) approaches in which the external command input was used as the instrument. While such IV methods are non-iterative and produce unbiased estimates, they are suboptimal in the sense that the variance of the estimates does not approach the Cramer-Rao lower bound [13].

System identification using closed-loop data has been extensively studied in the control systems literature using parametric methods [14], [15]. One of the main conclusions in [14] is that unbiased, efficient estimates of a system operating in feedback may be obtained directly from closed-loop data, provided that the prediction error method (PEM) [13] is used with a suitably chosen (parametric) model structure. The model structure, as shown in Fig. 1, includes two subsystems: the deterministic dynamics, which map the controlled input to the measured output, and the noise model, which explains the noise in the measured output as the result of filtering an unmeasured white noise sequence through a stable, invertible filter. The inclusion of a noise-model in the closed-loop identification allows one to separate the contributions due to the external input from those due to noise propagating around the feedback loop.

While these parametric methods have been effective for control, physiological studies often require nonparametric methods to minimize the *a priori* assumptions that need to be made regarding the structure of the system under study. Such nonparametric identification methods are often used to identify models of joint dynamics, as they can more readily

handle systems that have either long delays, or multiple delayed components (either of which can occur if reflexes are significant), than methods based on low-order parametric models. In contrast, there is little to be gained by using nonparametric noise models. In this paper, we will develop an algorithm for identifying a system consisting of a finite impulse response (FIR) model of the deterministic dynamics, and an Auto-Regressive Moving Average (ARMA) noise model. The prediction error will be shown to be linear in the tap-weights that describe the FIR filter, but nonlinear in the parameters of the ARMA noise model. Thus, a separable least squares algorithm will be used to identify the optimal parameters of both the deterministic and noise systems. This paper provides the details of this algorithm and evaluates its performance by estimating the dynamics of a simple mechanical system operating inside a feedback loop. Results of a pilot limb impedance study are also presented. Preliminary versions of some of these results have been presented in abstract form [16].

II. Theory

A. Deterministic and Noise Models

Given N equally spaced samples of a system's input and output, $u(t)$ and $y(t)$, respectively, the objective of a system identification is to construct a model that predicts $y(t)$, based on $u(t)$, and perhaps the previous values of the output [13]. If the output is expected to be a possibly noise corrupted but otherwise linear function of the input, then the model structure shown in Fig. 1 can be used to describe the system,

$$y(t)=G(q)u(t)+H(q)e(t) \tag{1}$$

where $G(q)$ and $H(q)$ are (possibly infinite degree) polynomials in the backward shift operator, q^{-1}. The noise in the output measurement, $v(t) = H(q)e(t)$, is obtained by filtering an independent identically distributed (IID) sequence of random variables, $e(t)$, with a stable and inversely stable filter, $H(q)$.

In the control systems literature, it is common to estimate both $G(q)$ and $H(q)$. Given estimates, $\hat{G}(q)$ and $\hat{H}(q)$, of the plant and noise models, the one step ahead prediction error is given by [13]:

$$\varepsilon(t)=\widehat{H}^{-1}(q)\left(y(t)-\widehat{G}(q)u(t)\right) \tag{2}$$

The prediction error method (PEM) uses an iterative optimization based approach to find estimates $\hat{G}(q)$ and $\hat{H}(q)$ that minimize the cost:

$$V_N=\frac{1}{2N}\sum_{t=1}^{N}\varepsilon^2(t) \tag{3}$$

Provided there is no under-modeling, minimizing V_N results in prediction errors that are white and uncorrelated with the input [13]. As such, the prediction error, $\varepsilon(t)$, can be regarded as an estimate of the innovation, $e(t)$.

In several fields, including biomechanics [1], it is common to fit only the deterministic system, $G(q)$. Provided there is no feedback from $y(t)$ to the input, $u(t)$ will be uncorrelated with $v(t)$, since it is independent of the innovation, $e(t)$. As such, omitting the noise model

will not bias the estimate of $G(q)$. Furthermore, if the deterministic system is modeled as a finite impulse response (FIR) filter, it can be fitted using linear regression [17].

B. Noise in Force and Position Signals

When constructing a model, such as the block diagram in Fig. 2, the noise source must be placed at the correct point in the feedback loop. In joint dynamics experiments, the effects of voluntary contractions can provide a significant source of noise. Depending on the configuration of the actuator, this noise will appear primarily in either the force or the position measurements. Muscle contractions apply forces to a system consisting of the limb and actuator. When the actuator is much stiffer than the limb, changes in muscle force do not alter joint position. Voluntary interventions therefore appear as noise in the measured forces. The effect of the voluntary contractions does not appear in the measured position, and is not fed back to the controller. As a result, open-loop methods may be used, provided the position is treated as the input, so that the disturbance appears in the output signal.

In contrast, if the limb is much stiffer than the actuator, then the effects of voluntary intervention will appear as noise in the measured position. Unlike the previous case, this "noise" is included in the signal that is fed back to the controller. Thus, the system must be analyzed as a closed-loop system. Under both of these extreme conditions, the effect of voluntary contractions appears predominantly in only one of the two measured signals. Provided the noisy measurement is treated as the system output, unbiased estimates of the joint impedance can be obtained.

However, in cases where the mechanical properties of the actuator are on the same order of magnitude as those of the limb, noise will appear on both of the measured variables. Again, some form of closed loop identification method must be used, but it must also be to deal with noise in the input signal. While it may be possible to extend the closed-loop approach developed in this paper to deal with such "errors in the variables" problems [18], it is beyond the scope of the present paper.

C. Closed Loop Identification

If the system is in a feedback loop, such as that shown in Fig. 2, then the assumption that $u(t)$ and $v(t)$ are uncorrelated no longer holds. Indeed, the input to $G(q)$ is given by:

$$u(t)=\frac{F_c(q)}{1+F_c(q)G(q)}r(t)-\frac{F_c(q)}{1+F_c(q)G(q)}v(t) \tag{4}$$

The correlation between the deterministic and noise inputs, $u(t)$ and $v(t)$, leads to a bias in the estimate of the deterministic part of the system when open loop methods are used [13]. However, Forssell and Ljung [14] demonstrated that unbiased estimates of both $G(q)$ and $H(q)$ could be obtained using PEM, provided that the control loop includes at least a one sample delay, and that both the deterministic and noise models are identified simultaneously.

The usual practice in the control systems literature, is to model the two sub-systems, $G(q)$ and $H(q)$, with recursive digital filters. While we will use a parametric description for $H(q)$, the deterministic dynamics will be modeled as a FIR filter. Thus,

$$G(q)u(t)=\sum_{k=0}^{T} g(k)u(t-k) \tag{5}$$

for some finite memory length T. The measurement noise will be an Auto-Regressive Moving-Average (ARMA) process, since its exact structure is not relevant for most biomechanics studies and the use of a parametric noise model greatly simplifies the identification process. The formulation of this model is given by

$$\begin{aligned} v(t)&=\frac{C(q)}{D(q)}e(t) \\ &=\sum_{k=1}^{n_c} c_k e(t-k) - \sum_{j=1}^{n_d} d_j v(t-j)+e(t) \end{aligned} \tag{6}$$

and the prediction errors will be given by:

$$\varepsilon(t)=\frac{D(q)}{C(q)}(y(t)-G(q)u(t)) \tag{7}$$

The objective is to find $C(q)$, $D(q)$ and $G(q)$, that minimize V_N in (3). In general, this is a nonlinear least squares optimization problem, and can only be solved using some form of iterative optimization. However, for any given choice of $C(q)$ and $D(q)$, the optimal $G(q)$ can be found in closed form, by using linear regression to fit a FIR filter between the filtered input and output,

$$u_f(t)=\frac{D(q)}{C(q)}u(t) \tag{8}$$

$$y_f(t)=\frac{D(q)}{C(q)}y(t) \tag{9}$$

Thus, the minimization of (3) can be split into two sub-problems. The first is a nonlinear minimization with respect to the parameters of the noise model,

$$\theta_{\boldsymbol{n}}=\begin{bmatrix} c_1 & \dots & c_{n_c} & d_1 & \dots & d_{n_d} \end{bmatrix} \tag{10}$$

which must be solved using iterative methods. Note that $c_0 = d_0 = 1$ are fixed, and hence not included in the parameter vector, $\boldsymbol{\theta_n}$. The second problem is a linear least squares regression, which must be repeated each time the estimate of $\boldsymbol{\theta_n}$ is updated, that is used to estimate the elements of the FIR filter, $G(q)$.

The nonlinear parameters are initialized to an initial guess. In practice, we set $C(q) = D(q) = 1$. Thus,

$$\theta_{\boldsymbol{n}}^{(\mathbf{0})}=\begin{bmatrix} 0 & 0 & \dots & 0 \end{bmatrix}^T \tag{11}$$

Then, an iterative search is used to find the optimal $\boldsymbol{\theta_n}$. For example, the nonlinear parameters can be updated using a Levenberg-Marquardt step [13]:

$$\theta_{\mathbf{n}}^{(\mathbf{j+1})}=\theta_{\mathbf{n}}^{(\mathbf{j})}+(\mathbf{J}^T\mathbf{J}+\delta\mathbf{I})^{-1}\mathbf{J}^T\varepsilon \tag{12}$$

where δ is a parameter that alters the convergence speed and stability of the iterative algorithm, and $\mathbf{J}$ is the Jacobian of the model output, a matrix with entries:

$$\mathbf{J}(t,k)=\frac{\partial\widehat{y}(t)}{\partial\theta_{\mathbf{n}}(k)} \tag{13}$$

The difficulty, is that changing the parameters in $\theta_{\mathbf{n}}$ can result in changes to the FIR filter. This dependency must be included in the partial derivatives.

Ruhe and Wedin [19] derived 3 algorithms for such separable problems (which include the separable least squares [20] problem as a special case). Let $\mathbf{J}_\ell$ be a matrix containing the partial derivatives of the prediction error with respect to the FIR filter coefficients, thus

$$\mathbf{J}_\ell(t,k)=\frac{\partial\varepsilon}{\partial g_k}=-u_f(t-k). \tag{14}$$

Similarly, let $\mathbf{J_n}$ be a matrix containing the partial derivatives of the prediction error with respect to the parameters of the noise model, assuming that the deterministic FIR dynamics remain fixed. The columns due to the numerator coefficients are:

$$\mathbf{J}_{\mathbf{n}}(t,k)=\frac{\partial\varepsilon}{\partial c_k}=\frac{-1}{C(q)}\varepsilon(t-k) \tag{15}$$

Similarly, the columns due to the denominator coefficients are:

$$\mathbf{J}_{\mathbf{n}}(t,n_c+k)=\frac{\partial\varepsilon}{\partial d_k}=\frac{1}{C(q)}(y(t-k)-G(q)u(t-k)) \tag{16}$$

Following Ruhe and Wedin [19], the Jacobian for the separated problem, where $G(q)$ is treated as a function of the noise model, can be approximated by:

$$\mathbf{J}=\mathbf{Q}_\ell\mathbf{J}_{\mathbf{n}} \tag{17}$$

where $\mathbf{Q}_\ell = \mathbf{I}-\mathbf{J}_\ell(\mathbf{J}_\ell{}^T\mathbf{J}_\ell)^{-1}\mathbf{J}_\ell{}^T$ is a projection orthogonal to the columns of the linear Jacobian, $\mathbf{J}_\ell$. This separated Jacobian can then be used in the Levenberg-Marquardt step (12).

It is possible to choose the value of δ in (12) such that the cost function, V_N, either decreases or remains constant after each iteration. As a result, it is possible to guarantee convergence to a local minimum. As with all gradient-based optimization schemes, one cannot guarantee that the minimum that was found is the global minimum.

III. Methods

A. Experimental

Details of the experimental apparatus have been reported previously [21], [22]. Briefly, a linear motor (Copley Thrust-Tube TB3806; Copley Controls, Canton, MA) was controlled using an admittance controller implemented on a PC running Matlab xPC (The Mathworks, Natick, MA). This system also was used for data collection. The actuator position was measured using a linear encoder (RGH24; Renishaw, Gloucestershire, UK) with a resolution of 1 μm, while applied forces and moments were measured by a load cell (67M25; JR3, Woodland, CA) attached to the actuator. This sensor has a force range of ±200N, and a moment range of ±12Nm with an accuracy of better than 0.05N. Motor control and data acquisition occurred at 5kHz. The analog force signals were sampled by a 16-channel, 16-bit data acquisition system (PCI-DAS1602/16; Measurement Computing, Middleboro, MA). Prior to sampling the force signals were anti-alias filtered using custom-built, differential input, 4th order Bessel filters with a cutoff frequency of 500 Hz.

The admittance controller simulated an environment consisting of mass, spring and damper:

$$H_e(s)=\frac{1}{M_e s^2+B_e s+K_e} \tag{18}$$

As shown in Fig. 3, the input to $H_e(s)$ was the force measured by the load cell. Its output, a stimulated position, was used as the command signal for the actuator, which was itself configured as a position servo. Thus, the actuator would produce a response that simulated interaction with the environment $H_e(s)$. Note that if the environmental stiffness is very large, then $H_e(s)$ has a near-zero gain, and the system approximates a pure position servo, tracking the input perturbation, $x_p(t)$.

In the configuration illustrated in Fig. 3, the input to the plant is a force (or torque), $f(t) + f_v(t)$, which produces an output position (or angle) signal, $x(t)$. Thus, these experiments directly identify the plant's admittance, $G(s)$, defined as the dynamic inverse of its impedance. This formulation was previously used by de Vlugt *et al.* [11], in their closed-loop investigations. The controller, $F_c(s)$ in Fig. 2, is realized using the feedback loop involving the actuator $H_{act}(s)$ and the virtual environment, $H_e(s)$. The signals $f_v(t)$ and $v(t)$ represent noises in the force and position measurements, respectively. As these are expected to be dominated by the effects of voluntary contractions, one can expect $v(t)$ to predominate when the controller is simulating a compliant environment, whereas $f_v(t)$ will be significant when a stiff controller is used, as discussed in Sec. II-B. Since $f_v(t)$ and $v(t)$ are likely to be non-white, they can each be modeled as the output of a noise model, as in Figs. 1 and 2.

B. Mechanical System

In one set of experiments, a pair of springs (260 N/m) and a mechanical damper (AirPot 2KS95; AirPot Corporation, Norwalk CT) were attached between the load cell and the frame surrounding the actuator, aligned with the linear motion of the actuator. This system was used to validate the results produced by the closed-loop identification technique, under a variety of virtual environments produced by the admittance controller.

The mass-spring-damper system was identified using a Gaussian white-noise perturbation, filtered with a second-order Butterworth low-pass filter with a cut-off frequency of 10 Hz. The filtered perturbation was then scaled so that it had a standard deviation of 0.5mm. This signal was sent as a position command, $x_p(t)$ in Fig. 3, to the admittance controller, which was set to simulate a critically damped mass-spring-damper system, with a virtual mass of M_e = 1 Kg, and spring constants of K_e = 50,000, 200, 10 and −200 N/m. The position measurement (which was also fed back to the controller) was corrupted with an independent Gaussian noise signal, filtered to a bandwidth of 5 Hz, and scaled so that the ratio of the command position to the position noise was 13 dB. Three trials were performed with each controller. Trials lasted 30 seconds, and were sampled at 5000 Hz. The input perturbation was zeroed for the first and last second of each trial, leaving 28 seconds of input/output data.

The data were decimated to obtain a sampling frequency of 200 Hz. Note that the decimation also included an 8'th order low-pass filtering, with a cut-off frequency of 80 Hz. Transients were removed from both ends of the data (due to the use of zero-phase filters), prior to the analysis. This left 4400 input/output data points, 3900 of which were used for identification, while the remaining 500 points were used for model validation.

C. Limb Impedance

In the second set of experiments, the linear motor was used to perturb the upper arm of a volunteer subject. The subject gave written informed consent and was free to withdraw at any time. The protocol was approved by the Northwestern University Institutional Review Board.

The motor was oriented orthogonal to the forearm and the upper limb was strapped into an adjustable trough to restrict motion to the elbow joint only. A custom-fitted fiberglass cast extending from the fingers to the middle of the forearm was used to maintain the wrist joint in a neutral position and to attach the forearm to the actuator via an aluminum plate epoxied under the cast and a precision bearing centered at the wrist. This configuration allowed rotation only in the horizontal plane.

The input perturbation was a white Gaussian noise signal, low pass filtered by a second-order Butterworth filter with a 5 Hz. cutoff frequency, and scaled so that its standard deviation was 3mm. This command signal was sent to the admittance controller, which was programmed to simulate one of two virtual mass, spring and damper systems. The stiff environment had a spring constant of K_e = 50 KN/m, whereas the compliant environment simulated a spring constant of K_e = 20 N/m. Both virtual systems included a 1.5 Kg mass, and a damping constant chosen to achieve critical damping.

The force measured by the load cell was low pass filtered, and presented to the subject on a monitor, together with a target force level of 0, 5, 10 or 15% of their maximum voluntary contraction (MVC). In most trials, the subject was instructed not to react to the perturbation, but to maintain the same contraction level throughout. In the last three trials, these instructions were reversed, and the subject was asked to attempt to compensate for the perturbation, and match the target level as closely as possible throughout the trial. These latter instructions were used to assess the influence of voluntary interventions, and the associated noise, on the estimation process.

D. Analytical Methods

In all cases, models were fit between the measured force and position signals using the direct closed-loop algorithm proposed herein. These models will be referred to as closed-loop FIR/ARMA models.

The model structure was determined empirically. Initially, a long impulse response with a high-order noise model was fitted. The prediction errors were checked for whiteness, and lack of causal correlation with the force signal. The IRF length and ARMA model orders were reduced until significant correlations were noted in the residuals, or between the residuals and past values of the input force signal, either of which would indicate omissions in the model structure. The final model structure included the shortest IRF length and lowest order ARMA noise model that produced acceptable residuals.

These models were compared to several alternate model types. Ordinary least squares was used to fit FIR filters with the same memory length as the FIR/ARMA models. These will be referred to as open-loop FIR models. To compare the predictive power of the open-loop FIR models and the closed-loop FIR/ARMA models, two intermediate models were also considered. First, the MATLAB system identification toolbox was used to fit an ARMA noise model, of the same order as that used in the closed-loop FIR/ARMA model, to the residuals resulting from the open-loop FIR model. These open-loop FIR/ARMA models could be directly compared to the closed-loop FIR/ARMA models, since they had identical structures (i.e. FIR filter lengths, ARMA model orders). Similarly, removing the noise model from a closed-loop FIR/ARMA model, results is an FIR model that had been identified using closed-loop techniques, which can then be compared directly to an open-loop FIR model.

For comparison purposes, models were also fitted using 2 standard approaches for closed-loop systems.

- A parametric Box-Jenkins model was fitted using the bj routine in the MATLAB system identification toolbox. Aside from the use of a recursive filter instead of a non-parametric impulse response, this model structure is the same as the FIR/ARMA structure proposed in this paper, so the two models may be compared directly.
- A FIR model was fit using the position command signal as an instrumental variable, using the technique described in [12]. As with the open-loop FIR model, the IV-FIR model was was augmented with an ARMA noise model, for comparison purposes.

The predictive power of the models was evaluated by comparing the mean squared errors (MSEs) of their outputs, evaluated on separate validation data which had not been used in the training of the models. These were then normalized with respect to the variance of the measured output, resulting in normalized mean squared errors (NMSEs).

IV. Results and Discussion

A. Mechanical System

When fitting the closed-loop FIR/ARMA model, as described above, the final models comprised a 151 sample (i.e. 0.75 second) IRF and a noise model with 11 poles and 10 zeros. In each case, the Levenberg-Marquardt algorithm converged in 20–25 iterations. Results from a typical trial are shown in Fig. 4. The upper panel shows the IRF of the system, while the lower panel plots the magnitude of the noise model's frequency response.

The residual correlations from this model are shown in the upper row of Fig. 5. The residuals appear to be white and not causally correlated with the input. The significant input/residual correlations at negative lags (note the large positive peak 1 sample to the left of $\tau = 0$) indicate the presence of feedback. When there is feedback (and the controller includes a delay), the current value of the controller output depends on past values of the measurement

noise. If the prediction errors are white, the current value of the prediction error will be uncorrelated with the past of the measurement noise, and hence with the current value (and past values) of the controller input. However, the current prediction error, that component of the measurement noise that cannot be predicted from its past values, will influence future values of the measurement noise, and hence future values of the controller output, generating this apparently anti-causal correlation between the prediction errors and the controller output/plant input.

When the open-loop algorithm was used (lower row), the noise model was still able to produce reasonably white residuals, as seen in the residual auto-correlation, but there were significant correlations, both causal and anti-causal, between the input and the residuals. Significant correlations between the past inputs and current residuals indicate that are errors in the FIR component of the model.

It was necessary to use a high-order noise model (11 poles, 10 zeros), in order to produce uncorrelated residuals. When lower order models were used, the residual auto-correlation contained several peaks outside of the 99% confidence bounds. The need for a high-order noise model is likely due in part to the effects of an 8'th order anti-aliasing filter used during decimation.

One should also note the sharp peak at 60 Hz, in the lower panel of Fig. 4. This is almost certainly power-line interference affecting the measured force signal (since it is the only analog measurement). Including the effects of this noise source likely added to the complexity of the noise model.

Several models were fitted to each dataset: open and closed loop FIR models and and open and closed loop FIR/ARMA models, as well as parametric Box-Jenkins models, and FIR/ARMA models fitted using an instrumental variable approach. The normalized mean squared prediction errors from each model structure, and each experimental trial, are plotted in Fig. 6. In all cases, the closed-loop FIR/ARMA model produced the smallest prediction errors. The FIR/ARMA models identified using either IV or open-loop least squares methods, produced NMSEs that were approximately 2–3 times larger. The Box-Jenkins model produced prediction errors that were about an order of magnitude larger than those due to the closed-loop FIR/ARMA model. In addition, the residual correlations, shown in the upper left panel of Fig. 7, indicated the presence of significant under-modeling. All of the models that included noise models significantly out-performed all of the models that did not.

The NMSEs reported in Fig. 6 should be interpreted with care. The FIR models all resulted in 3–4% NMSE in the validation data, which is consistent with the approximately 13 dB SNR expected in the data. The inclusion of a noise model dramatically reduced the NMSE in all cases. Ideally, this should result in prediction errors equal to the white noise source that was filtered and scaled to produce the measurement noise, and should therefore have the same variance in each experiment, which was nearly the case for the closed-loop FIR/ARMA models. The very small prediction error magnitudes can be be attributed to the relatively high sampling rate, 200 Hz after decimation, as compared to the 10 and 5 Hz bandwidths of the input and noise signals, respectively.

The left panel of Figure 7 compares the impulse responses (IRFs) of identified models of the mechanical system, averaged across all experimental trials. The IRF in the closed-loop FIR/ARMA model is the most likely to be correct, since the prediction errors due to this model were the smallest, see Fig. 6, and since they were not causally correlated with the control input. The input-residual correlations for the closed and open loop FIR/ARMA models are plotted in the right panels of Fig. 5, whereas those from the BJ and IV models appear in the

right panels of Fig. 7. The large input residual correlations in the open loop, BJ and IV models suggest that there are modeling errors or biases in their estimates of the deterministic subsystem, which show up as differences between these models and the IRF estimated using the closed-loop approach. In the case of the BJ model, this is likely due to an under-modeling of the system. The reported results used a second-order deterministic system, which would be expected for a mass-spring-damper. Although increasing the model order reduced the correlations, they could not be eliminated, at least with models of 20th order or less.

B. Elbow Dynamics

The FIR and FIR/ARMA model types were fit to the data resulting from the elbow experiments. In this case, the models included a 301 sample (1.5 second) FIR filter complemented with an ARMA noise model. When the stiff controller was used, an order (10,11) noise model was able to reproduce the noise spectrum. However, when the compliant controller was used, the order of the noise model had to be increased to (16,16). The prediction accuracy of these models was evaluated using the cross-validation data, and plotted in Fig. 8. Under all conditions, the closed-loop FIR/ARMA model provided the best predictions, followed by the open-loop FIR model augmented with an ARMA noise model. The closed-loop model often performed substantially better than even this model, sometimes by an order of magnitude. The two FIR-only models showed similar performance, one or two orders of magnitude worse than the models which included a noise component. The open-loop FIR model performed slightly better than the FIR component of the closed-loop model, under most conditions tested. Thus, the closed-loop FIR/ARMA model provided the best predictions, and this improvement is not simply due to the added parameters in the noise model, since better predictions were obtained when the FIR and ARMA components were identified simultaneously using separable least squares, rather than sequentially.

During the three trials displayed on the far right of Fig. 8, the subject was asked to react to the stimulus. As a result, the subject generated relatively large contractions, which were delayed beyond the memory length of the identified models. Although these voluntary contractions increased the size of the prediction errors, this increase was much less dramatic with the closed-loop algorithm than it was with the other models.

In addition to the open and closed-loop admittance models, open loop impedance models were also fitted to each trial. The impedance models were inverted, so that they could be compared to the FIR elements in the admittance models. Figure 9 shows Bode magnitude plots for the 3 models obtained from both Trials 11 (upper panel, $K_{env} = 50\ KN/m$) and 15 (lower panel, $K_{env} = 20\ N/m$). In both trials, the background contraction was 5% of MVC. In both cases, the deterministic part of the closed-loop FIR/ARMA model resembles a slightly underdamped, second-order system, with a resonant peak at about 2.5 Hz, and near constant gain at lower frequencies. These are consistent with the results reported in [23]–[25]. In both trials, the open-loop admittance models models captured the resonant peak, and subsequent roll-off, but also included unexpected dynamics at low frequencies. As expected, the inverse impedance model had reasonable dynamics when it was obtained in the stiff environment. However, the inverse impedance model contained unexpected low frequency dynamics when identified in the compliant environment. Thus, in addition to providing more accurate predictions than the other models, the closed-loop FIR/ARMA model was the only one that was also physically reasonable when identified in the compliant environment.

When the background contraction level was increased, similar results were noted in the compliant environment (not shown). In the stiff environment, the inverse stiffness continued to yield reasonable models, even when the background contraction level was increased to 10 or 15% MVC. However, the closed-loop admittance model began to show significant bias.

Again, this is expected since the noise in the stiff environment is largely present in the torque signal, which is the input to the admittance model. Once this noise level becomes significant, noticeable bias appears in the model.

Finally, statistical validation tests were applied to the closed-loop models, as discussed in Section III-D. Figure 10 shows the results from Trials 11 (upper 2 panels) and 15 (lower 2 panels). The grey rectangles represent 99% confidence bounds around zero. With one exception at $\tau \approx 0.45s$ in the upper plot, the residual autocorrelations (left) remain inside the 99% confidence bounds, shown as gray rectangles, indicating that the prediction errors are statistically equivalent to white noise, hence suggesting that the noise models are correct. Similarly the input/residual cross-correlations remain well inside the 99% bounds for $\tau \geq 0$, suggesting that the control input is uncorrelated with the past prediction errors, and hence that the deterministic systems is not missing any significant dynamics. The presence of much larger correlations at negative τ values suggests the presence of feedback.

When the background contraction level was increased to 10 and 15% MVC, the validation plots from the compliant trials remained essentially the same. However, in the stiff environment the residual correlations crossed significantly outside of the 99% confidence bounds (not shown), indicating bias in the models. In the stiff environment, we expected the effects of voluntary contractions to appear predominantly as noise in the torque signal, which is the input to the admittance model. Thus, we expected biased estimates in the stiff environment, and that the bias would increase with the level of background contraction.

V. Conclusions

An algorithm for the identification of FIR systems operating in closed loop was developed. It is a direct application of the prediction error approach, and includes an ARMA model of the prediction errors. This resulted in an optimization problem that could be solved efficiently using a separable least squares approach.

The algorithm was validated using an experimental study on a simple mechanical system operating in closed loop with a variable admittance controller. It was shown to produce unbiased estimates of the plant dynamics under all tested conditions, even when the measurement noise was non-white.

A pilot application to the study of joint dynamics in both stiff and compliant environments was undertaken. It was shown that the closed-loop algorithm could produce reliable estimates of joint dynamics under compliant conditions. Accurate estimates were also obtained under stiff conditions, but only when the background contraction was relatively low. In this case, the background contractions enter the system as a torque perturbation, which appears at the input to the plant admittance, and hence bias the resulting model. As the environment shifts from being compliant to being stiff, relative to the limb dynamics, the effect of voluntary contractions shift from the output to the input of the admittance model, resulting in biases in the resulting estimates. If the background contractions are relatively small, the bias may be insignificant. More sophisticated methods, likely based on total least squares, will be needed to deal with these intermediate cases, especially when the subject is producing relatively large contractions.

One limitation of the present study, is that the analysis is confined to linear systems. It is well known [1] that limb impedance can be strongly nonlinear. In the present study, a broad band excitation was used, as this is known to suppress the effects of reflexes [8], which are a major source of nonlinearity in the impedance. The present contribution is a necessary initial step in the development of a closed-loop nonlinear system identification algorithm, which

will be required in order to characterize the effects of reflexes as they interact with a wide variety of environments.

Acknowledgments

The authors would like to thank Mr. Tim Haswel for his assistance with the experiments. A MATLAB implementation of the identification algorithm is available from the first author.

This work was supported by the Natural Sciences and Engineering Research Council of Canada (grant RPGIN-238939-2005), and the National Institutes of Health (grants R01 NS053813 and R24 HD050821).

References

1. Kearney R, Hunter I. System identification of human joint dynamics. CRC Crit Rev Biomed Eng 1990;18:55–87.
2. Hunter I, Kearney R. Dynamics of human ankle stifness: variation with mean ankle torque. J Biomech 1982;15:747–752. [PubMed: 7153227]
3. Kearney R, Hunter I. Dynamics of human ankle stiffness: variation with displacement amplitude. J Biomech 1982;15:753–756. [PubMed: 7153228]
4. Cannon S, Zahalak G. The mechanical behavior of active human skeletal muscle in small oscillations. J Biomech 1982;15(2):111–121. [PubMed: 7076686]
5. Trumbower R, Krutky M, Yang BS, Perreault E. Use of self-selected postures to regulate multi-joint stiffness during unconstrained tasks. PLoS ONE May;2009 4(5):e5411. [PubMed: 19412540]
6. Gomi H, Osu R. Task-dependent viscoelasticity of human multijoint arm and its spatial characteristics for interaction with environments. J Neurosci 1998;18(21):8965–8978. [PubMed: 9787002]
7. Perreault E, Kirsch R, Crago P. Multijoint dynamics and postural stability of the human arm. Exp Brain Res August;2004 157(4):507–517. [PubMed: 15112115]
8. Kearney R, Stein R, Parameswaran L. Identification of intrinsic and reflex contributions to human ankle stiffness dynamics. IEEE Trans Biomed Eng 1997;44(6):493–504. [PubMed: 9151483]
9. Doemges F, Rack P. Task-dependent changes in the response of human wrist joints to mechanical disturbance. J Physiol 1992;447:575–585. [PubMed: 1593461]
10. Dietz V, Discher M, Trippel M. Task-dependent modulation of short- and long-latency electromyographic responses in upper limb muscles. Electroen Clin Neuro 1994;93:49–56.
11. de Vlugt E, Schouten A, van der Helm F. Closed-loop multivariable system identification for the characterization of the dynamic arm compliance using continuous force disturbances: a model study. J Neurosci Meth 2003;122(2):123–140.
12. Ravichandran V, Perreault E, Westwick D, Cohen N. Nonparametric identification of the elbow joint stiffness under compliant loads. Proc IEEE Eng Med Biol Conf 2004;26:4706–4709.
13. Ljung, L. System Identification: Theory for the User. 2. Upper Saddle River, NJ: Prencice Hall; 1999.
14. Forssell U, Ljung L. Closed-loop identification revisited. Automatica 1999;35:1215–1241.
15. Gustavsson I, Ljung L, Soderstrom T. Identification on processes in closed loop - identifiability and accuracy aspects. Automatica 1977;13:59–75.
16. Westwick D, Perreault E. Unbiased identification of finite impulse response linear systems operating in closed-loop. Proc IEEE Eng Med Biol Conf 2006;28:2118–2121.
17. Westwick, D.; Kearney, R. IEEE Press Series in Biomedical Engineering. Piscataway, NJ: IEEE Press/Wiley; 2003. Identification of Nonlinear Physiological Systems, ser.
18. Soderstrom T. Errors-in-variables methods in system identification. Automatica 2007;43:939–958.
19. Ruhe A, Wedin P. Algorithms for separable nonlinear least squares problems. SIAM Rev 1980;22(3):318–337.
20. Golub G, Pereyra V. The differentiation of pseudo-inverses and nonlinear least squares problems whose variables separate. SIAM J Num Anal 1973;10(2):413–432.

21. Lewis G, MacKinnon C, Perreault E. The effect of task instruction on the excitability of spinal and supraspinal reflex pathways projecting to the biceps muscle. Exp Brain Res 2006;174:413–425. [PubMed: 16676166]

22. Shemmel J, An J, Perreault E. The differential role of motor cortex in stretch reflex modulation induced by changes in environmental mechanics and verbal instruction. J Neurosci 2009;29(42):13 255–13 263.

23. Mirbagheri M, Alibiglou L, Thajchayapong M, Rymer W. Muscle and reflex changes with varying joint angle in hemiparetic stroke. J NeuroEng & Rehabil 2008;5(1):6. [PubMed: 18304313]

24. Perreault E, Kirsch R, Acosta A. Multiple-input, multiple-output system identification for characterization of limb stiffness dynamics. Biol Cybern 1999;80:327–337. [PubMed: 10365425]

25. Zhang L, Rymer W. Simultaneous and nonlinear identification of mechanical and reflex properties of human elbow joint muscles. IEEE Trans Biomed Eng 1997;44(12):1192–1209. [PubMed: 9401219]

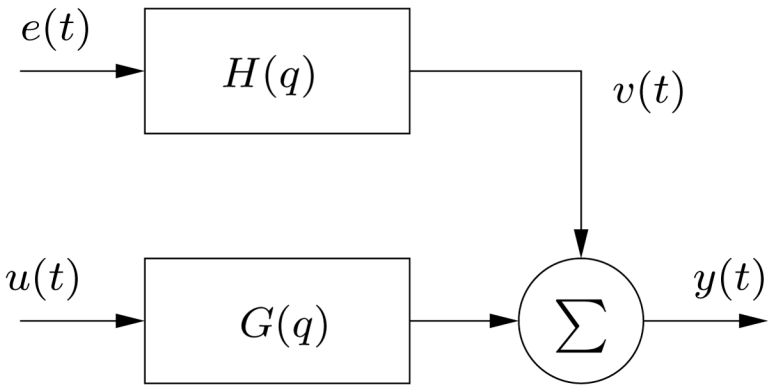

Fig. 1.
Complete model of a linear system showing both the deterministic subsystem, and the noise model. The experimenter is assumed to have access to $u(t)$ and $y(t)$. The innovation input, $e(t)$ is an unmeasurable sequence of independent, identically distributed random variables.

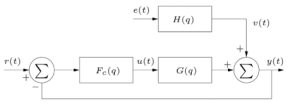

Fig. 2.
Block diagram of a linear feedback system, where $G(q)$ and $H(q)$ are the plant and noise models, and $F_c(q)$ is the controller.

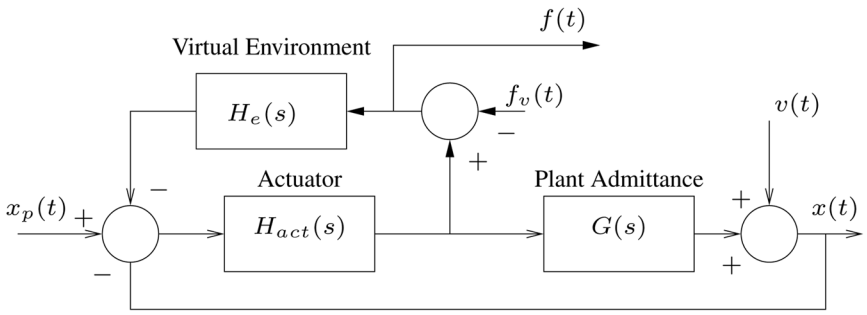

Fig. 3.

Block diagram of an admittance control loop. The inputs are $x_p(t)$, the perturbation to the position command, that was used to identify the system, and $f_v(t)$ and $v(t)$, which are the disturbances, primarily due to voluntary contractions, in the force and position measurements, respectively. The measurements are $f(t)$, the force measured by the load cell, and $x(t)$, the position of the actuator. The admittance controller is realized using the inner feedback loop involving the Virtual Environment and the Actuator.

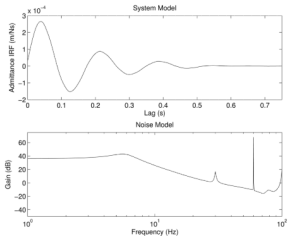

Fig. 4.

FIR/ARMA model identified for the mass-spring-damper system (M = 0.43 Kg, K = 520 N/m) operating in closed-loop. The upper panel shows the impulse response of the FIR model. The magnitude of the ARMA noise model gain is shown in the lower panel. Note that the innovation, $e(t)$, which is the unmeasured input to the noise model, has been arbitrarily assigned the same units as the measured position. Thus the gain is unitless.

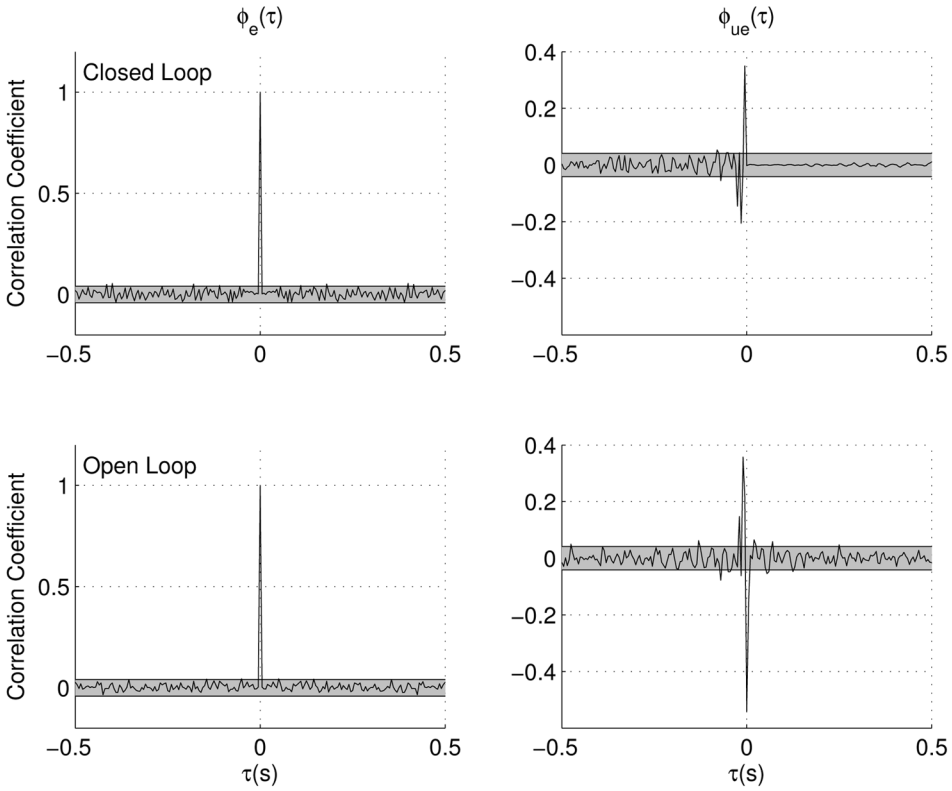

Fig. 5.

Residual correlations used to validate the FIR/ARMA models of the mechanical system identified using both open-loop (bottom row) and closed-loop (top row) approaches. The shaded regions show 99% confidence bounds around zero.

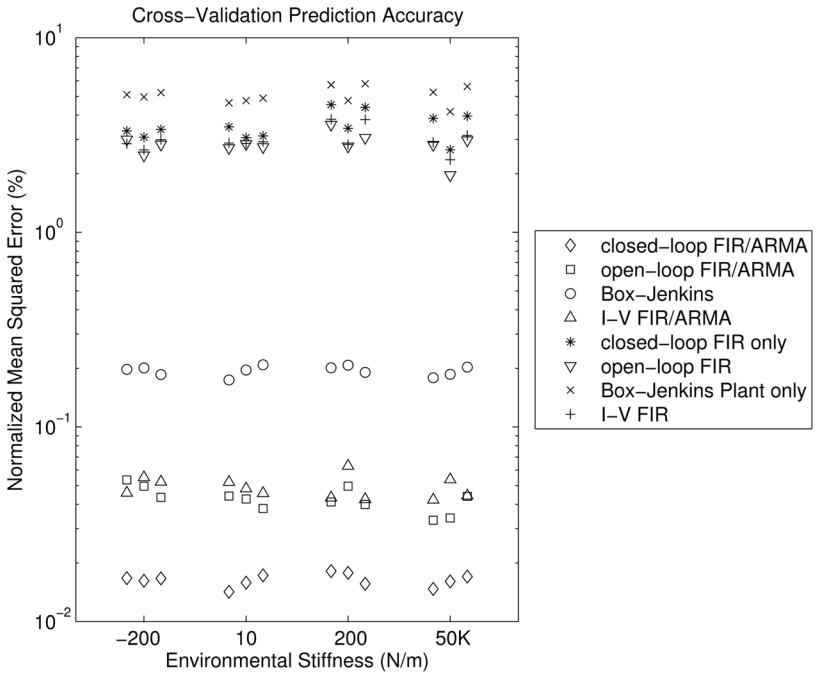

Fig. 6.

Prediction accuracy in validation data. Under all conditions tested, the FIR/ARMA model produced significantly more accurate predictions than any of the other model structures.

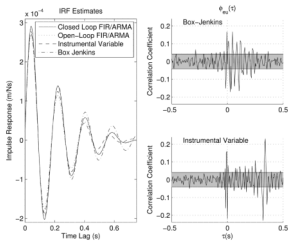

Fig. 7.

Impulse responses of the Mass-Spring-Damper system, estimated using the techniques reported in Fig. 6 (left) and the input-residual cross-correlations produced by the Box-Jenkins and Instrumental Variable models (upper and lower right, respectively).

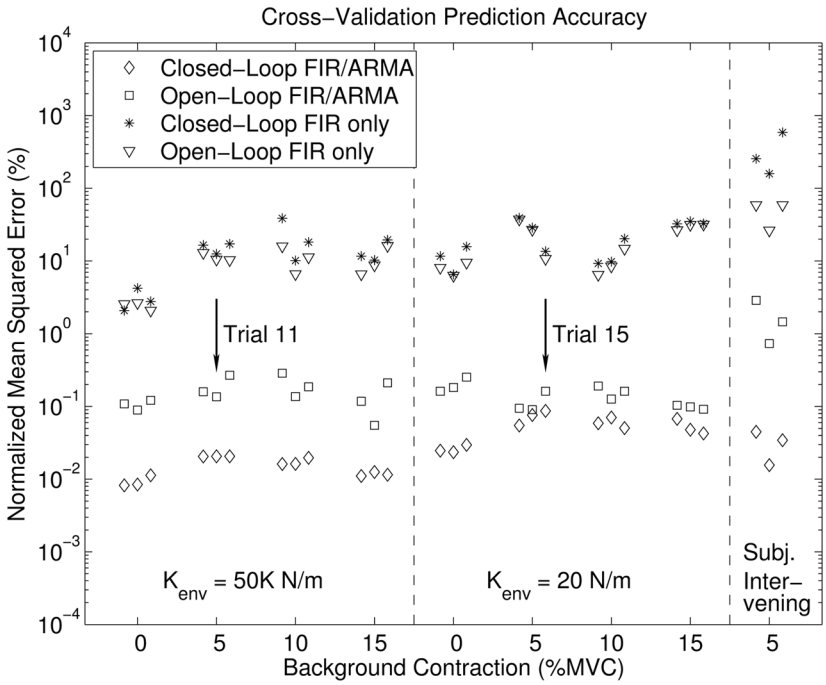

Fig. 8.

Prediction accuracy in the validation data. Trials are arranged in increasing order of contraction levels, with three trials each at 0, 5, 10 and 15% MVC. The 3 rightmost results were obtained in the compliant environment and a 5% MVC contraction, but unlike the rest of the trials, where the subject was instructed not to react to the perturbation, the subject was intervening throughout these trials. The arrows indicate the results from Trials 11 and 15, which are presented in detail in Figs. 9 and 10.

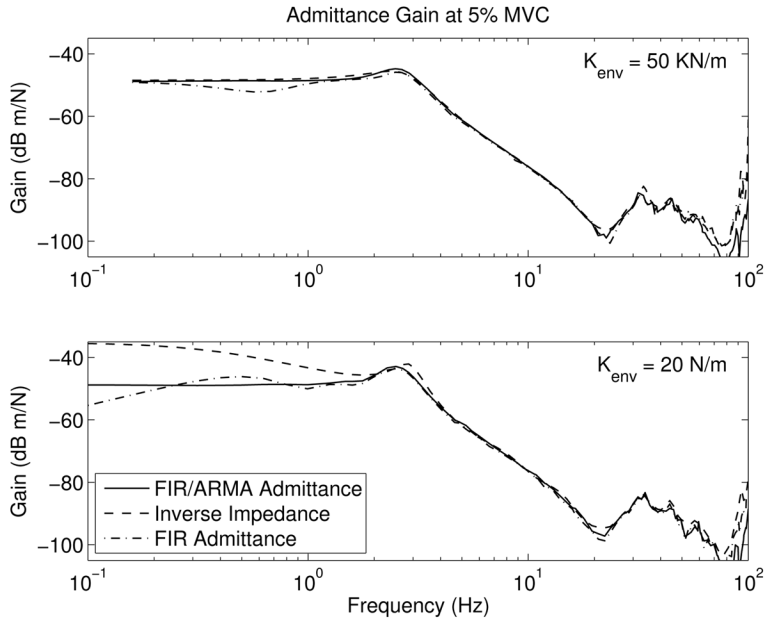

Fig. 9.
Models of elbow admittance, obtained from trials 11 (top panel) and 15 (lower panel)

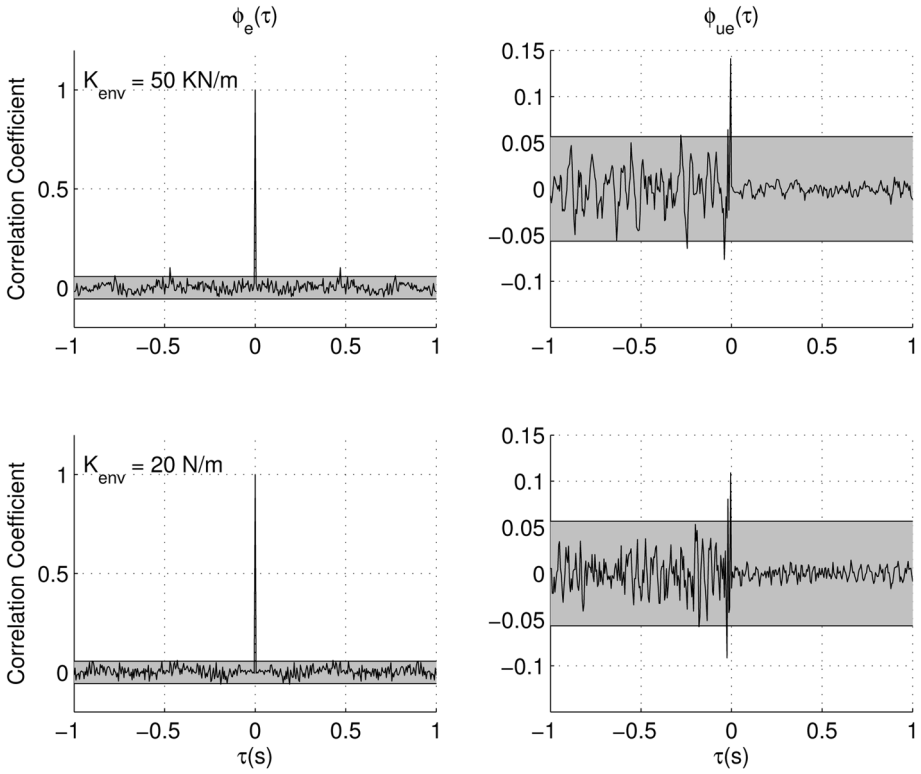

Fig. 10.

Correlation tests of model validity applied to the data from trials 11 (upper row) and 15 (lower row). The shaded regions show 99% confidence bounds around zero. The right hand panels show the auto-correlation of the prediction errors, while the lower panels show the cross-correlation between the input and the residuals. Significant correlations at negative lags indicate the presence of feedback.